Accepted Manuscript

Title: Performance of an activated carbon supercapacitor electrode synthesised from waste Compact Discs (CDs)

Authors: Rifat Farzana, Ravindra Rajarao, Badekai Ramachandra Bhat, Veena Sahajwalla

Please cite this article as: Rifat Farzana, Ravindra Rajarao, Badekai Ramachandra Bhat, Veena Sahajwalla, Performance of an activated carbon supercapacitor electrode synthesised from waste Compact Discs (CDs), Journal of Industrial and Engineering Chemistry https://doi.org/10.1016/j.jiec.2018.05.011

Performance of an activated carbon supercapacitor electrode synthesised from waste Compact Discs (CDs)

Rifat Farzana[a*], Ravindra Rajarao[a], Badekai Ramachandra Bhat[b], Veena Sahajwalla[a]

[a]Centre for Sustainable Materials Research and Technology (SMaRT)

School of Materials Science and Engineering, UNSW Sydney, Australia, NSW 2052.

[b]Catalysis and Materials Laboratory, Department of Chemistry, National Institute of Technology

Karnataka, Surathkal, D.K., Karnataka 575025, India.

Corresponding author: Rifat Farzana (r.farzana@unsw.edu.au)

Graphical abstract
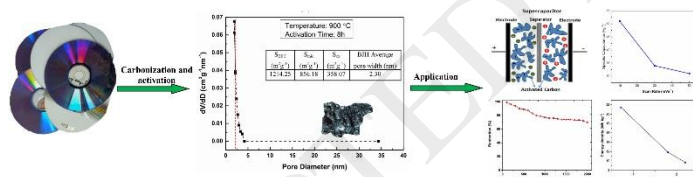
<u>Highlights</u>

• Novel route to synthesize activated carbon for supercapacitor electrode using waste CDs as precursor.

• Highest surface area of 1214.25 m^2g^{-1} was achieved at 900°C temperature and 8 hours

activation time.

• The electrochemical measurements of waste CDs derived activated carbon exhibited good specific capacitance (51 Fg^{-1}) and cycle stability (80%) compared to other waste derived activated carbon.

• This sustainable pathway will reduce the huge volumes of waste CDs in landfill and will create alternative resource for supercapacitor electrode.

Abstract

Microporous activated carbon was synthesised using waste compact discs as precursor through

physical activation method for supercapacitor electrode application. The activated carbon

prepared at 900 °C for a time interval of 8 hours showed highest surface area of 1214.25 $m^2 g^{-1}$.

The electrochemical measurements showed that waste CDs derived activated carbon exhibited

good specific capacitance, cycle stability and good rate capability compared to other waste

derived activated carbon. The specific capacitance 51 F g^{-1} at the current density of 10 mV s^{-1}

and energy density of 21.43 Wh kg^{-1} at power density 0.7 kW kg^{-1} was achieved in non-aqueous

electrolyte.

1. Introduction

Supercapacitors or electrochemical capacitors are electrical energy storage devices, which lie

between batteries and conventional dielectric capacitors in terms of energy and power densities

[1-3]. They offer higher power, better life cycle and higher reliability than batteries, but have much lower energy density and higher self-discharge. Hence, supercapacitors have applications in appliances such as electronic devices, electrical vehicles and military equipment's [4]. Supercapacitors primarily consist of electrodes, current collectors, electrolyte and a spacer. Electrodes which operates at the electrode/electrolyte interface are important as the power density and cyclability mainly depends on electrode properties [5-7]. Common materials used as supercapacitor electrode are activated carbons, conducting polymers, metal oxides/nitrides, graphene and carbon nanotube [8-10]. Activated carbon looks more promising compared to other materials due to its easy availability, low cost, high surface area, good electrical conductivity, good anti-causticity and high electrochemical stability [6, 11]. Activated carbons are mainly produced by physical activation or chemical activation by using coal, coke, carbonized organic precursor or char as primary source. Chars produced by pyrolysis and coal/coke consist of elementary crystallites with large number of interstices which concurrently lower the extent of porosity by blocking the pore entrance. In order to increase surface area of char or coal, chemical or physical activation process (steam or CO_2) is performed through a controlled carbon burn off and elimination of volatiles [11, 12]. Carbon precursor, activation temperature and time greatly influence the properties of activated carbon such as pore size distribution and surface area [11]. Activated carbons are traditionally produced from petroleum coke, pitch and coals, but the scarcity of fossil fuels has recently stimulated an interest in researchers to investigate inexpensive precursors [8]. One of the main challenges for activated carbon commercial manufactures is to identify new precursors that are inexpensive and easily available. Therefore, a lot of studies has been performed to produce activated carbons by using waste materials such as polymeric waste including rubber tyre, polystyrene, polyethylene terephthalate bottles, PCB [13-

3

17] and other bio-waste [8, 12, 18-24]. Hence, exploring an alternative waste source for producing activated carbon will provide an alternative source for the application in electrodes fabrication for supercapacitors.

Compact discs (CDs) or digital versatile discs (DVDs) are portable storage for recording, storing and playing audio, video or other digital data. Estimated production of CDs and DVDs worldwide was 12 billion pieces in 2003 [25] and has increased significantly in recent years. Waste CDs have contributed significantly to landfill due to the complex nature of manufacturing process (approximately 10% of all manufactured CDs are rejected), postconsumer CDs and destruction of CDs because of artist's right issue (unsold copies) [25]. Every year, nearly 5.5 million CDs go to landfills and incinerators and millions of CDs are discarded [26]. Recycling of waste CDs is a complex process and tedious due to its heterogeneous combination of polymer and multi-layer metal layer [27]. Recently, we have evaluated the structure of char and gas generation during pyrolysis of waste CDs as valuable supplementary carbon source for ironmaking industries and also reported the utilization for waste CDs to synthesise nano silicon carbide [27, 28].

In this present study, waste CDs was used as resource to prepare microporous activated carbon. Microporous activated carbon was prepared by a one step process of carbonization followed by physical activation by CO_2. Various analytical techniques such as nitrogen adsorption desorption, scanning electron microscope (SEM), X-ray diffraction (XRD), X-ray photon spectroscopy (XPS) and Fourier transform infra-red (FTIR) spectroscopy were employed to study the properties of obtained activated carbons. In addition, electrochemical properties such as galvanostatic charge-discharge (GCD); cyclic voltammetry (CV) and electrochemical impedance spectroscopy (EIS) were carried to assess the capacitance properties of synthesized microporous

4

activated carbon. This study will help simultaneously to address environmental issue of waste CDs recycling and to create an economic solution by producing value-added microporous activated carbon for supercapacitor application.

2. Experimental

2.1 Materials and methods

Waste CDs, used in this study was picked up from the recycling unit of UNSW Australia, Sydney. Waste CDs were dried and pulverized manually to smaller pieces before the experiments. Ultimate analysis using LECO analyzer was conducted to detect major elements like carbon, nitrogen. To determine moisture, volatiles and ash content in waste CDs, proximate analysis was carried out. Wavelength dispersive X-ray fluorescence spectroscopy (WDXRF) was also performed using PANanalytical PW2400 Sequential WDXRF to determine various minor elements in waste CDs.

Fourier transform infrared spectroscopy (FTIR, Spectrum 100 PerkinElmer) measurement was conducted with a spectral range of 650 cm^{-1} to 4000 cm^{-1} to identify the polymer composition in waste CDs and compared with virgin polycarbonate material to verify the attribution of FTIR peaks.

Thermogravimetric analysis (TGA) of waste CDs was conducted by Simultaneous Thermal Analyzer (STA 8000, PerkinElmer) by heating sample from 30 ˚C to 700 ˚C in nitrogen (N_2) atmosphere, at a rate of 10 ˚C min^{-1}. Carbon content of char residue was measured by LECO carbon analyzer (LECO CS-444).

2.2 Preparation of activated carbon

Waste CDs were used to prepare activated carbons by a one step process of carbonization followed by activation. Waste CDs were cut into small pieces and pyrolyzed at 700 ˚C, 800 ˚C

and 900 ˚C for 15 minutes in argon gas atmosphere. Carbonization by pyrolysis enriches the

carbon content in char and initial porosity of waste CDs. After 15 minutes of pyrolysis, gas flow

was switched to CO_2 and pyrolyzed chars were activated at 700 ˚C, 800 ˚C and 900 ˚C

temperature respectively at different time intervals of 1, 3, 5 and 8 hours to enhance pore

structure. Carbonization by pyrolysis and activation process was simultaneously conducted as

one step process in laboratory scale horizontal tube furnace.

2.3 Methods for characterization of activated carbon

Porosity, pore volume and surface area of the produced activated carbons was determined using

N_2 adsorption at liquid nitrogen temperature (-196 ˚C) (TriStar 3000, V6.08 A). Adsorption data

were obtained over the relative pressure, P/P_0, range from 0 to 1. The samples were degassed at

150 ˚C under vacuum for 3 hours. The N_2 apparent surface area was calculated by using the

Brunauer-Emmett-Teller (BET) equation. The micropore surface area was determined by using t-

plot method by determining the slope (s) between the relative pressure and volume adsorbed data

($S_{micro} = S_{BET} - S_{ext}$, where $S_{ext} = s \times 15.47 \, m^2 \, g^{-1}$). Mesopore volume and diameter was

determined by Barrett-Joyner-Halenda (BJH) method.

Structural and chemical properties of the activated carbon obtained from waste CDs were

determined by X-ray diffraction (XRD, PAN analytical Xpert Multipurpose MPD), Scanning

Electron Microscopy (SEM, Hitachi 3400-I), X-ray photoelectron spectroscopy (XPS,

ESCALAB250Xi, Thermo Scientific), FTIR (Spectrum 100 PerkinElmer) and Raman

Spectroscopy (Renishaw inVia) techniques.

2.4 Method for electrochemical characterization

The capacitive behavior of waste CDs derived activated carbon electrodes for supercapacitor were evaluated using electrochemical methods including cyclic voltammetry (CV), galvanostatic charge-discharge (GCD) measurement and electrochemical impedance spectroscopy (EIS) using electrochemical workstation of Autolab Potentiostat / Galvanostat (Model- PGSTAT 30, Ecochemie, The Netherlands). Two electrode configuration, by using waste CD derived activated carbon electrode separated by a thin polypropylene separator and electrolyte of 1-Ethyl-3-Methylimidazolium Tetra-fluoroborate (EMIMBF4) was used. The CV tests were carried out with a wide voltage range of 0 to 3 V at different scan rates varying from 10 mV s^{-1} to 50 mV s^{-1}. The gravimetric specific capacitance, C_{sp} (F g^{-1}), was calculated according to **equation 1 [29]**,

$C_{sp} = 2 (Q_+ + |Q_-|) / 2m\Delta V$…………………………….. equation (1)

Here, Q_+ is the integrated charge of anodic potential, Q_- is the integrated charge of cathodic potential, m is the mass of individual electrode and ΔV is the potential window (for this work $\Delta V = 3V$).

The GCD measurements were carried out at various applied currents (2.85, 7.1 and 8.5 A g^{-1}) in order to investigate the capacitive behavior. By using chronopotentiometry, specific capacitance C_{sp} (F g^{-1}), was calculated by according to the following **equation 2** [24, 29].

$C_{sp} = 2 \times I / m (\Delta V / \Delta t)$………………………………….. equation (2)

Here, I (A) denote discharge current, m (g) is the mass of material of individual electrode, ΔV (V) is the change in potential during the discharge process, Δt (s) is the discharge duration. Due to the symmetric capacitor assembly of the materials factor 2 is incorporated.

7

The energy density E (Wh kg^{-1}) and power density P (kW kg^{-1}) were evaluated using following **equations 3 and 4 [29]**.

E = 1000 C_{sp} ΔV^2 / 4×2×3600……………………………. equation (3)

Here, C_{sp} is the cell specific capacitance, ΔV is the cell voltage (iR drop corrected).

P = E / T_d ………………………………………………….equation (4)

Here, T_d denote the discharging time.

3. Results and Discussion

3.1 Characterization of waste CD

CDs are a multi-layered product consisting of thermoplastic polycarbonate substrate with a thin layer of metal coating. Polycarbonate resin is widely used in manufacturing CD due to its properties such as exceptional clarity, light transmittance, low moisture absorption and high impact strength [25]. **Figure 1** shows the polycarbonate structure and FTIR stretching of different functional groups of waste CD. FTIR spectra of waste CD showed C−H group (~ 2970 cm^{-1}), triplet peaks of C−O group (~ 1166 cm^{-1}, 1194 cm^{-1}, 1228 cm^{-1}), strong C=O group (~1700 cm^{-1}), aromatic groups by its overtones (~1506 cm^{-1}) and 'oop' bands. As the spectrum of waste CD matched the pure polycarbonate peaks, it confirms that the waste CDs used for this study is fabricated by using polycarbonate polymer.

Figure 1

The elemental analysis of waste CD is shown in **Table 1**. Ultimate and proximate analysis shows that waste CD contains high amount of carbon with minimal amount of ash. Ash content can be attributed to silica which is the highest concentration in elemental analysis. Volatiles in waste CD is high (77.99 wt%) and at 600 ˚C temperature volatiles are removed which can be confirmed by TGA analysis shown in **Figure 2(a)** where 73% weight loss was observed. The

8

degradation of waste CD started around ~ 500 ˚C and almost completed at ~ 600 ˚C which was clearly observed from TGA curve, and hence the temperature for carbonization and activation was chosen above 600 ˚C. **Figure 2(b)** shows the carbon yield from 600 ˚C to 900 ˚C. At 600 ˚C char yield was ~27% and from temperature 700 ˚C to 900 ˚C char yield decreased slightly 23% to 21%. Decreasing trend of char yield could be attributed to the primary or secondary decomposition in char residue at higher temperatures and transformation into carbon [27, 30].

Table 1

Figure 2

3.2 Characterization of activated carbon

(a) N$_2$ adsorption isotherm

Figure 3a is showing the adsorption-desorption isotherms of activated carbon obtained from waste CD at different activation temperature of 700 ˚C, 800 ˚C and 900 ˚C. The isotherms for the activated carbon at 900 ˚C is of type 1 according to the IUPAC classification [31] and completely overlapped without showing any hysteresis loop. The reversible type 1 isotherm of concave shape is characteristic of the presence of microporous structure with a narrow pore size distribution. Nonappearance of hysteresis loop also represents the absence of 'ink-bottle' shaped pores forms due to capillary condensation [32]. At relatively low pressures, high volume adsorptions were observed because of narrow pore width and the high adsorption potential. However, slightly upswept rear edge at high relative pressure (P/P$_0$ > 0.9), suggests the existence of mesopores as well [33]. Therefore, it can be concluded that activated carbon prepared in this work is dominantly comprises of micropores with few mesopores as well. Activated carbon at

9

700 ˚C and 800 ˚C exhibit adsorption isotherm of type IV, with slight hysteresis which suggests the presence of mesopores/macropores along with micropores [33, 34].

Activation conditions such as time and temperature plays an important role on the porous structure of the activated carbon [35]. Activated carbon obtained at highest activation temperature of 900 ˚C showed highest development of the microporous structures. **Figure 3b** shows the adsorption-desorption isotherms of activated carbon obtained at different activation (1, 3, 5 and 8 hours) time duration at 900 ˚C. It was observed that increasing the duration of activation from 1 to 8 hours, increases the micro-porosity, concurrently higher volume of adsorption and shows type 1 characteristics without hysteresis loop.

Figure 3

The BET surface area and porosity parameters are shown in **Figure 4**. It was observed that activated carbon obtained by using waste CD at highest temperature (900 ˚C) exhibited larger surface area compared to 700 ˚C or 800 ˚C (**Figure 4a**). This rise in BET surface area followed the increasing trend with increasing temperature over time. Activated carbon at 900 ˚C and activation time 8 hours showed the highest surface area (1214.25 $m^2 g^{-1}$) in comparison of activated carbon obtained at 700 ˚C (602.94 $m^2 g^{-1}$) or 800 ˚C (1033.83 $m^2 g^{-1}$).

According to IUPAC, adsorbent pores are classified into micropores (< 2 nm), mesopores (2 to 50 nm) and macropores (> 50 nm). In **Figure 4b**, activated carbon obtained from waste CD at 900 ˚C temperature and 8 hours, time showed less than 50 nm pore size, which confirm the presence of micro and mesopores. Using t-method, surface area of micropores (S_{mic}) and mesopores (S_{ex}) was also determined. It was observed that micropores area was higher than the

10

mesopores area and average BJH pore width was 2.30 nm which also confirm the microporosity of the activated carbon.

Figure 4

(b) SEM analysis

Low and high magnification SEM images of activated carbon (Temperature: 900 °C, Time: 8 hours) is shown in **Figure 5**. The surface of the activated carbon clearly shows the regular microporosity and homogenous structure of carbon. Both higher surface area and microporosity are beneficial to the performance of supercapacitor, which would facilitate the electron/ion transfer process into the electrode. Therefore activated carbon prepared from waste CD, can be used as an input material for supercapacitors.

Figure 5

(c) XRD and Raman analysis

Activated carbon of highest surface area (Temperature: 900 °C, Time: 8 hours) was structurally characterized by XRD and Raman spectroscopy (**Figure 6**). The XRD pattern in **Figure 6a** showed a hump at lower angle ($2\theta=10\text{-}20°$) which indicated that major part of carbon in amorphous, and presence of pores which scatter the X-ray radiation [15] . The major peak of activated carbon was observed at $2\theta=44°$, corresponds to (100) plane of carbon structure [36] and indicates limited extent of crystallinity which is consistent with the diffused peak observed at 26°. Also the asymmetric nature of (002) peak is attributed to the low scattering angles due to presence of γ-band and is associated with the amorphous structure and/or irregularity in aromatic structures packing [37]. The (100) peak attributed to two dimensional reflection of X-ray from carbon layers, which also describes the aromatic part of the carbon structure [27].

11

Further structural details were obtained from Raman spectroscopy in **Figure 6b.** For carbon

materials valuable information can be obtained within wave number range 800 and 2000 cm^{-1}

[38]. The broad bands at ~1600 cm^{-1} is called G band, corresponding to the stretching vibration

in graphene layer i.e C=C sp^2 bonds. The other band located at ~1350 cm^{-1} is the D band is

associated with disordered graphite lattice due to the breathing mode of hexagonal rings and is

the more intense, the lower structural ordering.   Furthermore a peak related to random structure,

hides under valley between two peaks which reflects the presence of amorphous carbon. In this

study, the I_V/I_G ratio (I_V is intensity of a valley between G and D bands and I_G is intensity of G

band) is been used as an indication to measure the degree of disorder and proportion of

amorphous carbon. The I_V/I_G ratio of activated carbon was found 0.52 which is higher than

graphitic carbon [27] and represents the less crystalline and highly amorphous content of carbon.

Figure 6

(d) FTIR analysis

FTIR spectra of raw waste CD and activated carbon from waste CD (Temperature: 900 °C, Time:

8 hours) is shown in **Figure 7**. The peaks due to carbon dioxide have been subtracted to avoid

the interference from atmosphere during measurement. In activated carbon all peaks of waste CD

(C−H group, triplet peaks of C−O group, C=O group, aromatic groups by its overtones and oop

bands) disappeared (**Figure 7**) and looked similar to carbonaceous materials like coke [27]. Only

minor hump at ~1070 cm^{-1} was observed which is attributed to the C−O stretching. The absences

of functional groups in activated carbon confirm that the carbonate groups or aromatic structures

were completely degraded during pyrolysis along with activation process and transformed into

activated carbon.

Figure 7

(e) XPS analysis

Figure 8 and **Table 2** shows the XPS analysis results of the activated carbon obtained from waste CD (Temperature: 900 ˚C, Time: 8 hours). Carbon, oxygen and silicon were observed in XPS and the binding energy for carbon, oxygen and silicon are within 281.28~294.58, 526.88~537.98 and 98.28~104.48 respectively (**Table 2**). XPS spectra of C1s (**Figure 8a**) excitation showed complex envelope of several carbon species at the carbon surface (C1s A to C1s F). The major component (C1s A) was observed at binding energy of 284.44 eV with atomic concentration of 48.54%. The characteristic band of carbon C1s A generally belongs to graphitic peak [27, 39, 40]. Other peaks corresponds to C−C/C−H bonds (285.0 eV) for B, C−O bonds (286.48 eV) for C, C=O bonds (288.30 eV) for D, COO bonds (288.98 eV) for E and O−C=O bonds (290.50 eV) for F [40-42] in **Figure 8a**. However, depending on the chemical nature of the neighboring atoms on individual surface, the peak position may shift slightly. The O1s spectra represent the presence of three peaks of O1s A, O1s B and O1s C in **Figure 8b.** Peak O1s A corresponds to oxygen atom in carboxyl group (533.9 eV), O1s B corresponds to carboxylic (C=O) group (530.7 eV) and O1s C corresponds to oxygen atom in hydroxyls [40]. The trace amount of silicon peak Si2p A with atomic concentration 0.41% (**Table 2, Figure 8c**) is attributed to the presence of silicon dioxide (SiO_2) impurity in the waste CD.

Figure 8

Table 2

3.3 Electrochemical Performance of activated carbon from waste CD

Figure 9a shows the cyclic voltammograms (CVs) of the electrode made by activated carbon

from waste CD scanned at 10, 30 and 50 mV s^{-1} and its corresponding specific capacitance

values are 51, 34 and 31 F g^{-1}. The ideal CVs curve with rectangular shape validates excellent

capacitive behavior. Therefore, CVs curve, with slight deviation from rectangular shape, using

waste CD electrode demonstrates good capacitive behavior. The CV curves show larger area of

rectangle with increasing scan rates which demonstrate an increase in specific capacitance in

non-aqueous electrolyte. Even at lower scan rate (10 mV s^{-1}) CV curve did not show a very

narrow area which indicates better capacitance behavior [43-45]. Galvanostatic charge discharge

curve (GCD) is shown in **Figure 9b** for current densities 2.85, 7.1 and 8.5 A g^{-1}. It is noted that,

due to the limited diffusion of the active ions on the electrode surface, with increasing current

densities, the specific capacitance decreases [45]. The GCD curve shows minor asymmetric

triangular shape which can be attributed to the presence of more functional group and/or higher

IR drop in the electrode sample [45]. However, good linear response of cell potential over time

demonstrates good reversibility of the electrochemical change/discharge process [46]. The

variation of specific capacitance with scan rate of waste CD derived microporous activated

carbon is also represented in **Figure 9c.**

Figure 9

The stability of the activated carbon electrode was investigated by performing CV at a scan rate

of 100 mV s^{-1} for 2000 cycles and corresponding results are shown in **Figure 10a**. The specific

capacitance was around more than 80% up to 800 cycles and gradually decreases to 70% at 2000

cycles. The 80% retention up to 800 cycles indicates excellent cycle stability of the obtained

microporous activated carbon from waste CD.

14

By using **equation (3) and (4)**, energy density and power density was calculated by using specific capacitance (C_{sp}) and discharging time. C_{sp} is capacity based on single electrode, hence total capacity is 1/2 capacity of a single electrode. In equation (3), the factor 4 is incorporated in denominator because total electrode mass is twice of single electrode. The Ragone plot (relationship between energy density and power density) is represented in **Figure 10b**. The increase of power density with decrease in energy density is general phenomenon. In this work, activated carbon derived from waste CD showed best performance with high energy density of 21.43 Wh kg^{-1} at power density 0.7 W kg^{-1} and gradually reduces to 9.68 Wh kg^{-1} at power density 2.2 W kg^{-1}. The waste CD derived activated carbon electrode showed higher energy density and power density compare to commercial available supercapacitor electrodes which are in the range of energy density 4–5 Wh kg^{-1} with power density of 1–2 W kg^{-1}[29, 47].

The electrochemical impendence spectroscopy (EIS) measurement was carried out and its corresponding Nyquist plot is as shown in **Figure 10c**. The impendence spectroscopy was performed to determine the contact resistance, charge transfer resistance and diffusion resistance in pores of electrolyte ions during electrochemical process. EIS measurements were carried out in the frequency range from 100 K Hz to 10 M Hz. In this technique, at different frequency alternating current is applied at open circuit potential to examine the penetration ability of ions.

The Nyquist plot showed straight line in the low frequency region and small arc in the higher frequency which is typical behavior of supercapacitor. The small arc in the high frequency region clearly indicates the porous electrodes. The diameter of semicircle is directly related to the resistance of electrode and resistance between electrode and current collector. The smaller semicircle concludes that lower internal resistance is exhibited by the waste CD derived activated carbon electrode. This also indicates that the electrolyte ions pass through microporous

15

activated carbon very effectively. The line with steeper slope also indicates that the obtained

activated carbon from waste CD has uniform microporous structure [48]. The activated carbon

obtained by using waste CD exhibited good specific capacitance, cycle stability and good rate

capability because of the following properties; (a) higher surface area which provides surface

sites to form electrical double layer (b) uniform microporous pores give easy access for

electrolyte ions to pass through electrodes and hence lower diffusion resistance.

Figure 10

Table 3 summarizes the surface area and specific capacitance values for activated carbons

derived from various sources including wastes in non-aqueous electrolyte. It was observed from

literature that specific capacitance values vary from 18 to ~100 F g^{-1} [42, 49] and in our study,

waste CD derived activated carbon showed specific capacitance value of 51 F g^{-1} with surface

area of 1214 $m^2 g^{-1}$.

Table 3

4. **Conclusions**

This study concludes that waste CD can be used as precursor to produce uniform microporous

activated carbon for supercapacitor electrode application. The following conclusions were

obtained from this study:

(a) Highest surface area of 1214.25 $m^2 g^{-1}$ was achieved at 900 ˚C temperature and 8 hours

activation time.

(b) Nitrogen adsorption shows that the activated carbons obtained are essentially microporous

with an average BET surface area. XPS, SEM, FTIR, XRD and Raman analysis indicates that

16

properties of prepared activated carbon from waste CD could be used as input material for supercapacitors.

(c) The activated carbon obtained by using waste CD exhibited good specific capacitance, cycle stability and good rate ability. The specific capacitance 51 F g^{-1} at the current density of 10 mV s^{-1} was achieved.

(d) Energy density of 21.43 Wh kg^{-1} at power density 0.7 W kg^{-1} and 9.68 Wh kg^{-1} at power density 2.2 W kg^{-1} was also achieved by the prepared activated carbon from waste CD.

(e) This innovative approach of using waste CD activated carbon as supercapacitor electrode reduces the environmental burden of waste CDs and creates an alternative material for supercapacitor application.

Acknowledgements

References

[1] S. Faraji, F.N. Ani, The development supercapacitor from activated carbon by electroless plating—A review, Renewable and Sustainable Energy Reviews 42 (2015) 823-834.
[2] J. Gamby, P.L. Taberna, P. Simon, J.F. Fauvarque, M. Chesneau, Studies and characterisations of various activated carbons used for carbon/carbon supercapacitors, Journal of Power Sources 101 (2001) 109-116.
[3] S. Zheng, X. Li, B. Yan, Q. Hu, Y. Xu, X. Xiao, H. Xue, H. Pang, Transition-Metal (Fe, Co, Ni) Based Metal-Organic Frameworks for Electrochemical Energy Storage, Advanced Energy Materials (2017).
[4] R. Farma, M. Deraman, A. Awitdrus, I.A. Talib, E. Taer, N.H. Basri, J.G. Manjunatha, M.M. Ishak, B.N.M. Dollah, S.A. Hashmi, Preparation of highly porous binderless activated carbon electrodes from fibres of oil palm empty fruit bunches for application in supercapacitors, Bioresource Technology 132 (2013) 254-261.
[5] L. Timperman, A. Vigeant, M. Anouti, Eutectic mixture of Protic Ionic Liquids as an Electrolyte for Activated Carbon-Based Supercapacitors, Electrochimica Acta 155 (2015) 164-173.
[6] K. Wang, N. Zhao, S. Lei, R. Yan, X. Tian, J. Wang, Y. Song, D. Xu, Q. Guo, L. Liu, Promising biomass-based activated carbons derived from willow catkins for high performance supercapacitors, Electrochimica Acta 166 (2015) 1-11.

[7] P. Geng, S. Zheng, H. Tang, R. Zhu, L. Zhang, S. Cao, H. Xue, H. Pang, Transition Metal Sulfides Based on Graphene for Electrochemical Energy Storage, Advanced Energy Materials (2018).

[8] E. Redondo, J. Carretero-González, E. Goikolea, J. Ségalini, R. Mysyk, Effect of pore texture on performance of activated carbon supercapacitor electrodes derived from olive pits, Electrochimica Acta 160 (2015) 178-184.

[9] M.-S. Balogun, Y. Huang, W. Qiu, H. Yang, H. Ji, Y. Tong, Updates on the development of nanostructured transition metal nitrides for electrochemical energy storage and water splitting, Materials Today 20 (2017) 425-451.

[10] H. Pang, X. Li, Q. Zhao, H. Xue, W.-Y. Lai, Z. Hu, W. Huang, One-pot synthesis of heterogeneous Co3O4-nanocube/Co(OH)2-nanosheet hybrids for high-performance flexible asymmetric all-solid-state supercapacitors, Nano Energy 35 (2017) 138-145.

[11] A.G. Pandolfo, A.F. Hollenkamp, Carbon properties and their role in supercapacitors, Journal of Power Sources 157 (2006) 11-27.

[12] C. Bouchelta, M.S. Medjram, O. Bertrand, J.-P. Bellat, Preparation and characterization of activated carbon from date stones by physical activation with steam, Journal of Analytical and Applied Pyrolysis 82 (2008) 70-77.

[13] P. Ariyadejwanich, W. Tanthapanichakoon, K. Nakagawa, S.R. Mukai, H. Tamon, Preparation and characterization of mesoporous activated carbon from waste tires, Carbon 41 (2003) 157-164.

[14] K. Laszlo, A. Szűcs, Surface characterization of polyethyleneterephthalate (PET) based activated carbon and the effect of pH on its adsorption capacity from aqueous phenol and 2, 3, 4-trichlorophenol solutions, Carbon 39 (2001) 1945-1953.

[15] W. Bratek, A. Świątkowski, M. Pakuła, S. Biniak, M. Bystrzejewski, R. Szmigielski, Characteristics of activated carbon prepared from waste PET by carbon dioxide activation, Journal of Analytical and Applied Pyrolysis 100 (2013) 192-198.

[16] M. Zhi, F. Yang, F. Meng, M. Li, A. Manivannan, N. Wu, Effects of pore structure on performance of an activated-carbon supercapacitor electrode recycled from scrap waste tires, ACS Sustainable Chemistry & Engineering 2 (2014) 1592-1598.

[17] R.R. Rajagopal, L. Aravinda, R. Rajarao, B.R. Bhat, V. Sahajwalla, Activated carbon derived from non-metallic printed circuit board waste for supercapacitor application, Electrochimica Acta 211 (2016) 488-498.

[18] E. Köseoğlu, C. Akmil-Başar, Preparation, structural evaluation and adsorptive properties of activated carbon from agricultural waste biomass, Advanced Powder Technology 26 (2015) 811-818.

[19] D. A, G. Hegde, Activated carbon nanospheres derived from bio-waste materials for supercapacitor applications - a review, RSC Advances 5 (2015) 88339-88352.

[20] C. Zhan, X. Yu, Q. Liang, W. Liu, Y. Wang, R. Lv, Z.-H. Huang, F. Kang, Flour food waste derived activated carbon for high-performance supercapacitors, RSC Advances 6 (2016) 89391-89396.

[21] H. Laksaci, A. Khelifi, M. Trari, A. Addoun, Synthesis and characterization of microporous activated carbon from coffee grounds using potassium hydroxides, Journal of Cleaner Production 147 (2017) 254-262.

[22] A. Zubrik, M. Matik, S. Hredzák, M. Lovás, Z. Danková, M. Kováčová, J. Briančin, Preparation of chemically activated carbon from waste biomass by single-stage and two-stage pyrolysis, Journal of Cleaner Production 143 (2017) 643-653.

[23] N.A. Rashidi, S. Yusup, A review on recent technological advancement in the activated carbon production from oil palm wastes, Chemical Engineering Journal 314 (2017) 277-290.

[24] I.I.G. Inal, S.M. Holmes, E. Yagmur, N. Ermumcu, A. Banford, Z. Aktas, The supercapacitor performance of hierarchical porous activated carbon electrodes synthesised from demineralised (waste) cumin plant by microwave pretreatment, Journal of Industrial and Engineering Chemistry (2017).

[25] R. Zevenhoven, L. Saeed, Automotive shredder residue (ASR) and compact disc (CD) waste: options for recovery of materials and energy, Helsinki Univ. of Technology, Espoo (Finland) (2003) 74.

[26] R.K. Irshad Ahmed MANSURI, Ravindra RAJARAO and Veena SAHAJWALLA, Recycling Waste CDs as a Carbon Resource: Dissolution of Carbon into Molten Iron at 1 550 °C, ISIJ INternational 53 (2013) 2259–2265.

[27] R. Rajarao, I. Mansuri, R. Dhunna, R. Khanna, V. Sahajwalla, Study of structural evolution of chars during rapid pyrolysis of waste CDs at different temperatures, Fuel 134 (2014) 17-25.

[28] R. Rajarao, I. Mansuri, R. Dhunna, R. Khanna, V. Sahajwalla, Characterisation of gas evolution and char structural change during pyrolysis of waste CDs, Journal of Analytical and Applied Pyrolysis 105 (2014) 14-22.

[29] L. Aravinda, K. Nagaraja, H. Nagaraja, K.U. Bhat, B.R. Bhat, ZnO/carbon nanotube nanocomposite for high energy density supercapacitors, Electrochimica Acta 95 (2013) 119-124.

[30] R. Farzana, R. Rajarao, V. Sahajwalla, Transforming waste plastic into reductants for synthesis of Ferrosilicon alloy, Industrial & Engineering Chemistry Research 53 (2014) 19870-19877.

[31] S. Lowell, J.E. Shields, M.A. Thomas, M. Thommes, Characterization of porous solids and powders: surface area, pore size and density, Springer Science & Business Media2012.

[32] D.M. Ruthven, Principles of adsorption and adsorption processes, John Wiley & Sons1984.

[33] W. Si, J. Zhou, S. Zhang, S. Li, W. Xing, S. Zhuo, Tunable N-doped or dual N, S-doped activated hydrothermal carbons derived from human hair and glucose for supercapacitor applications, Electrochimica Acta 107 (2013) 397-405.

[34] X.Y. Chen, H. Song, Z.J. Zhang, Y.Y. He, A rational template carbonization method for producing highly porous carbon for supercapacitor application, Electrochimica Acta 117 (2014) 55-61.

[35] E. David, J. Kopac, Activated carbons derived from residual biomass pyrolysis and their CO2 adsorption capacity, Journal of Analytical and Applied Pyrolysis.

[36] I.I. Misnon, N.K.M. Zain, R.A. Aziz, B. Vidyadharan, R. Jose, Electrochemical properties of carbon from oil palm kernel shell for high performance supercapacitors, Electrochimica Acta 174 (2015) 78-86.

[37] P. Fu, S. Hu, J. Xiang, L. Sun, P. Li, J. Zhang, C. Zheng, Pyrolysis of maize stalk on the characterization of chars formed under different devolatilization conditions, Energy & Fuels 23 (2009) 4605-4611.

[38] A. Sadezky, H. Muckenhuber, H. Grothe, R. Niessner, U. Pöschl, Raman microspectroscopy of soot and related carbonaceous materials: Spectral analysis and structural information, Carbon 43 (2005) 1731-1742.

[39] J. Xu, L. Chen, H. Qu, Y. Jiao, J. Xie, G. Xing, Preparation and characterization of activated carbon from reedy grass leaves by chemical activation with H 3 PO 4, Applied Surface Science 320 (2014) 674-680.

[40] K. László, E. Tombácz, K. Josepovits, Effect of activation on the surface chemistry of carbons from polymer precursors, Carbon 39 (2001) 1217-1228.

[41] G.M. Burke, D.E. Wurster, M.J. Berg, P. Veng-Pedersen, D.D. Schottelius, Surface characterization of activated charcoal by x-ray photoelectron spectroscopy (XPS): Correlation with phenobarbital adsorption data, Pharmaceutical research 9 (1992) 126-130.

[42] T.A. Centeno, M. Hahn, J.A. Fernández, R. Kötz, F. Stoeckli, Correlation between capacitances of porous carbons in acidic and aprotic EDLC electrolytes, Electrochemistry Communications 9 (2007) 1242-1246.

[43] R. Liu, E. Liu, R. Ding, K. Liu, Y. Teng, Z. Luo, Z. Li, T. Hu, T. Liu, Facile in-situ redox synthesis of hierarchical porous activated carbon@ MnO 2 core/shell nanocomposite for supercapacitors, Ceramics International 41 (2015) 12734-12741.

[44] S. Hu, S. Zhang, N. Pan, Y.-L. Hsieh, High energy density supercapacitors from lignin derived submicron activated carbon fibers in aqueous electrolytes, Journal of Power Sources 270 (2014) 106-112.

[45] B. Lu, Z. Xiao, H. Zhu, W. Xiao, W. Wu, D. Wang, Enhanced capacitive properties of commercial activated carbon by re-activation in molten carbonates, Journal of Power Sources 298 (2015) 74-82.

[46] Y. Cai, B. Zhao, J. Wang, Z. Shao, Non-aqueous hybrid supercapacitors fabricated with mesoporous TiO2 microspheres and activated carbon electrodes with superior performance, Journal of Power Sources 253 (2014) 80-89.

[47] A. Burke, R&D considerations for the performance and application of electrochemical capacitors, Electrochimica Acta 53 (2007) 1083-1091.

[48] I.I.G. Inal, S.M. Holmes, A. Banford, Z. Aktas, The performance of supercapacitor electrodes developed from chemically activated carbon produced from waste tea, Applied Surface Science 357 (2015) 696-703.

[49] D. Lozano-Castelló, D. Cazorla-Amorós, A. Linares-Solano, S. Shiraishi, H. Kurihara, A. Oya, Influence of pore structure and surface chemistry on electric double layer capacitance in non-aqueous electrolyte, Carbon 41 (2003) 1765-1775.

[50] D. Hulicova, M. Kodama, H. Hatori, Electrochemical performance of nitrogen-enriched carbons in aqueous and non-aqueous supercapacitors, Chemistry of materials 18 (2006) 2318-2326.

[51] M. Domingo-García, J. Fernández, M. Almazán-Almazán, F. López-Garzón, F. Stoeckli, T. Centeno, Poly (ethylene terephthalate)-based carbons as electrode material in supercapacitors, Journal of Power Sources 195 (2010) 3810-3813.

[52] K. Kuratani, K. Okuno, T. Iwaki, M. Kato, N. Takeichi, T. Miyuki, T. Awazu, M. Majima, T. Sakai, Converting rice husk activated carbon into active material for capacitor using three-dimensional porous current collector, Journal of Power Sources 196 (2011) 10788-10790.
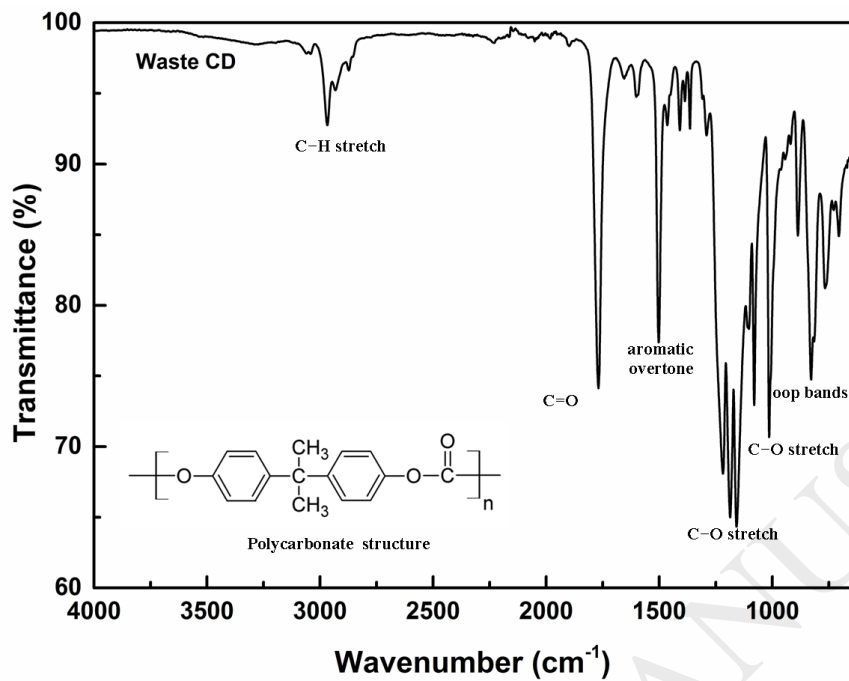
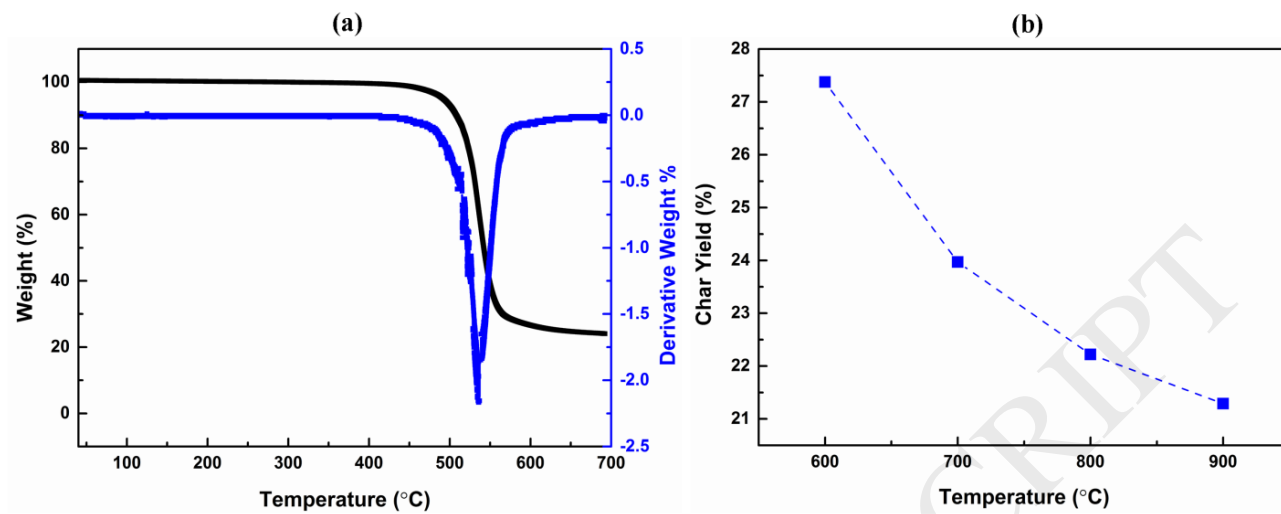**Figure 1:** Polycarbonate structure and FTIR spectrum of waste CD.

Figure 2: (a) TGA and DTG curves of waste CD and (b) char yield of waste CD at different
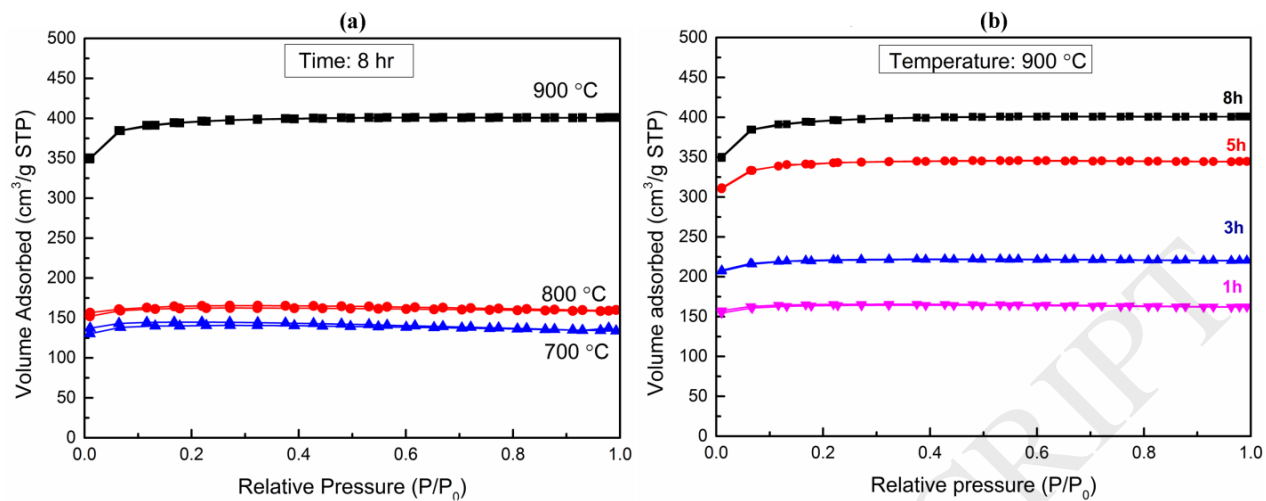
temperatures.

Figure 3: Nitrogen adsorption-desorption isotherms of (a) obtained activated carbons from waste

CD at different temperature and (b) activated carbons obtained at 900 °C for different time.
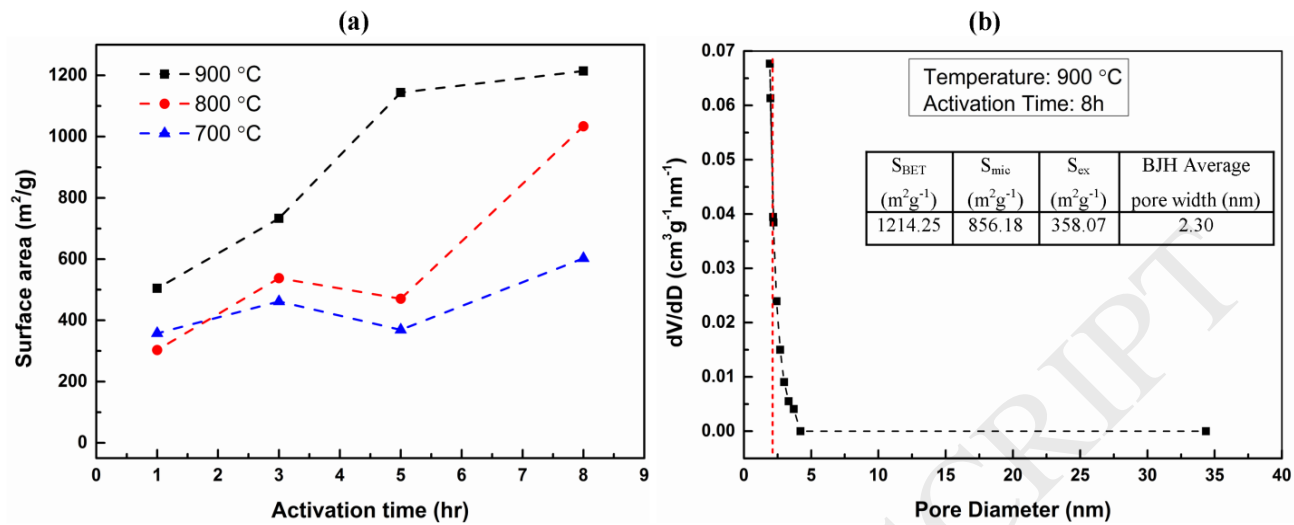
(a)

(b)

S_{BET} (m^2g^{-1})	S_{mic} (m^2g^{-1})	S_{ex} (m^2g^{-1})	BJH Average pore width (nm)
1214.25	856.18	358.07	2.30

Figure 4: (a) BET surface area and (b) Pore size distribution of activated carbons from waste CD at 900 ˚C for 8 hours.
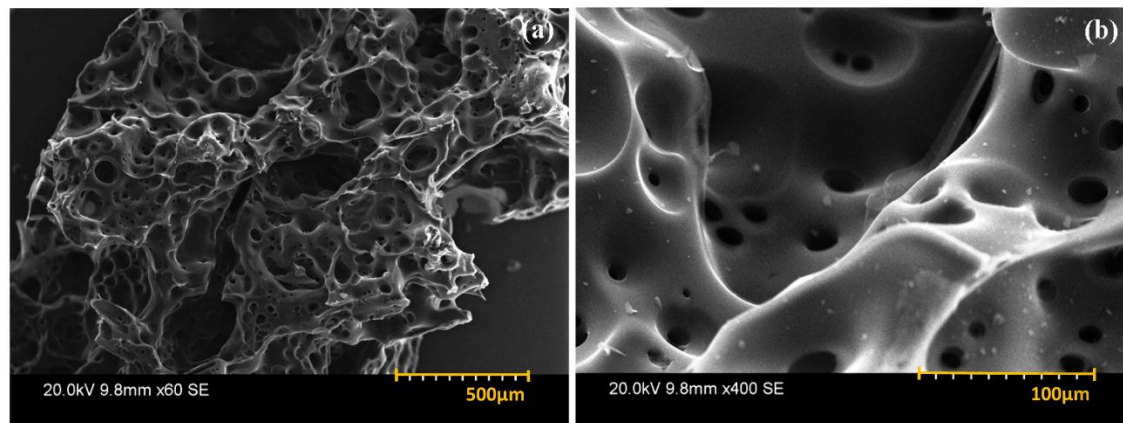
Figure 5: (a) Low magnification and (b) high magnification of Scanning electron micrograph of CO_2 activated carbon at 900 ˚C for 8 hours.
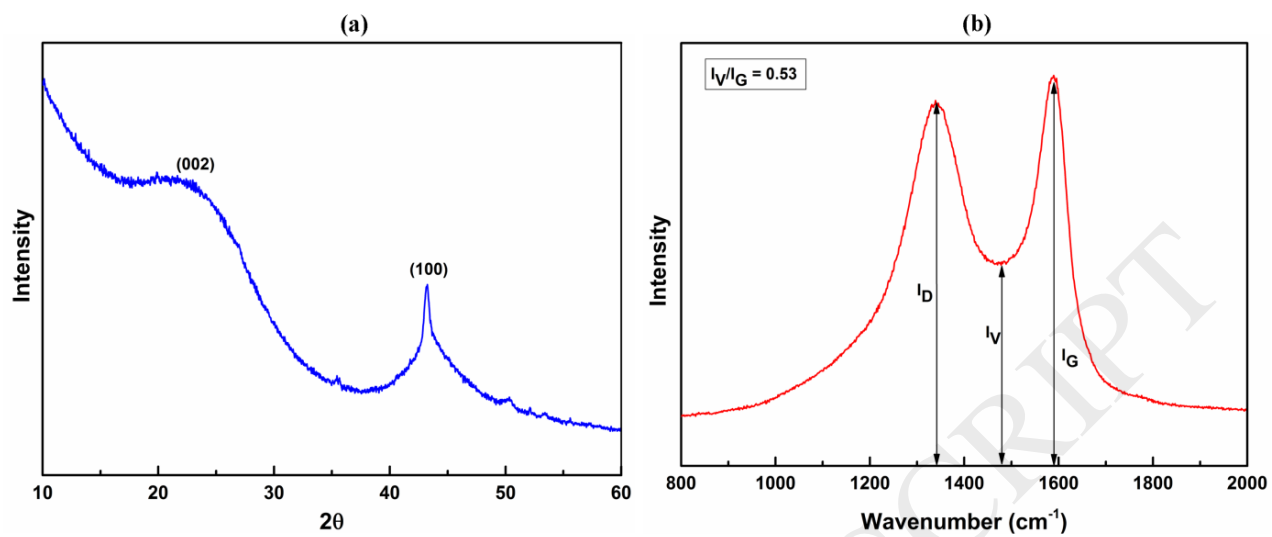
25

Figure 6: (a) XRD and (b) Raman spectra of activated carbon from waste CD activated at 900 ˚C for 8 hours.
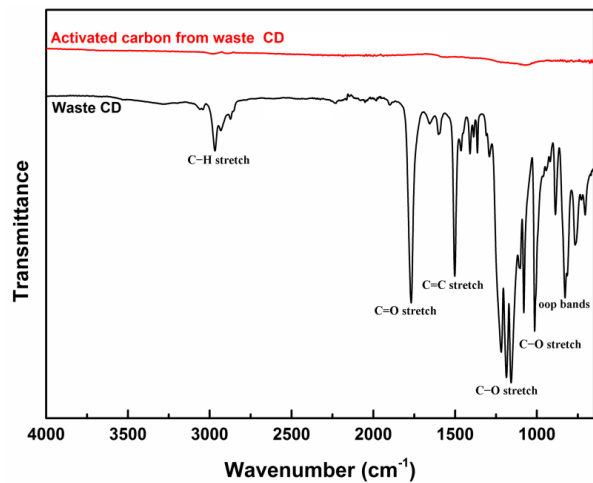
Figure 7: Comparison of FTIR spectra of raw CD and activated carbon from waste CD at 900 ˚C for 8 hours.
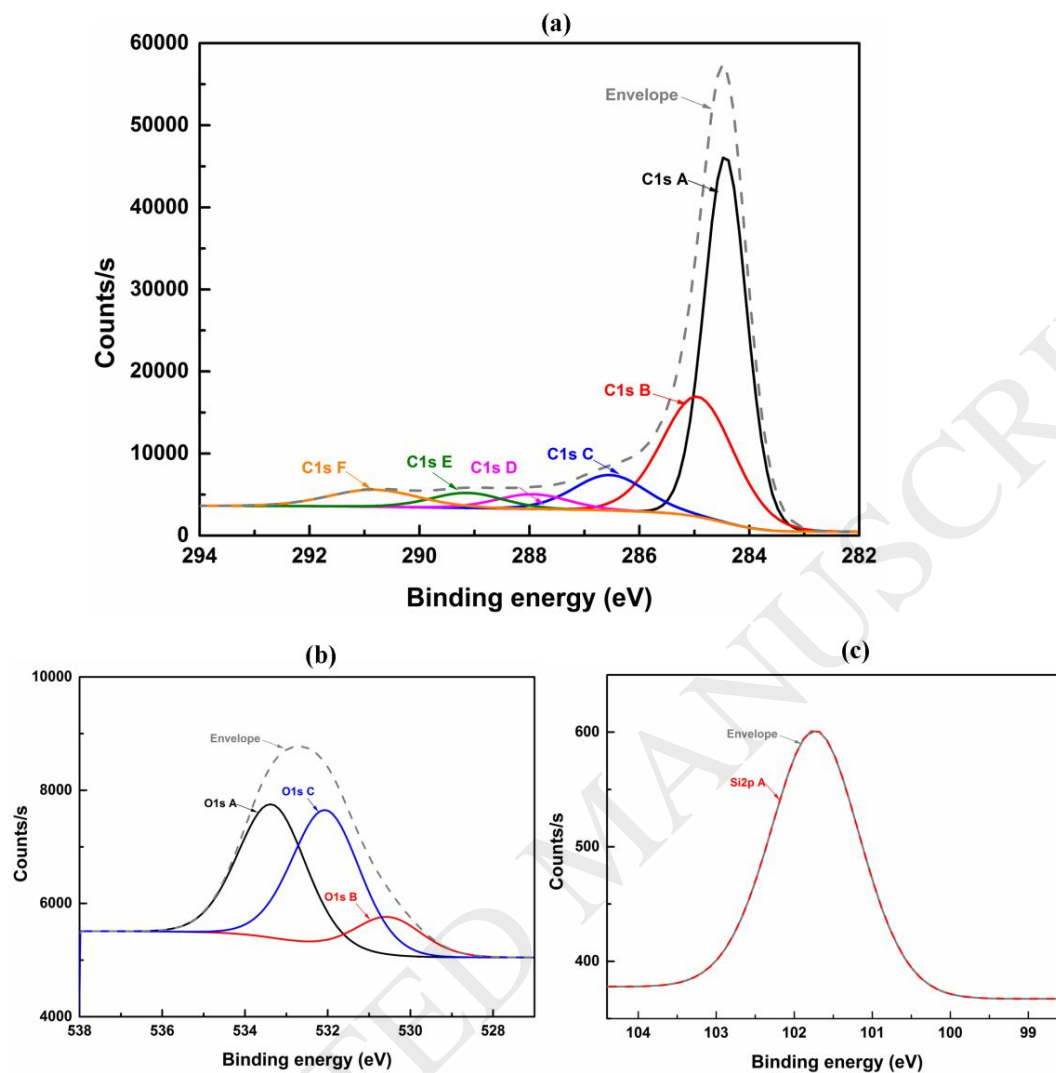
Figure 8: (a) C1s (b) O1s and (c) Si2p XPS spectra of activated carbon from waste CD at 900 ˚C for 8 hours.
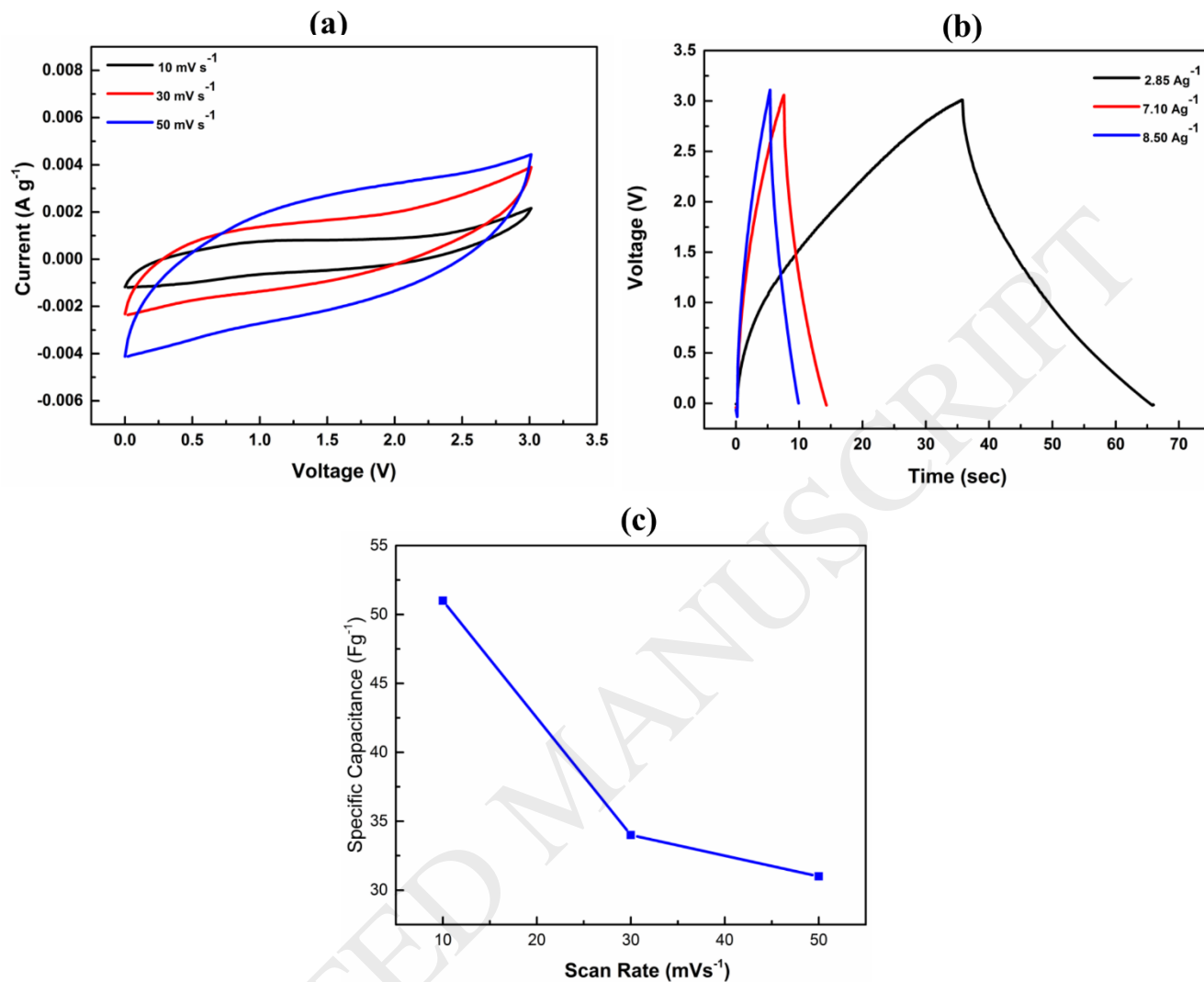
Figure 9: (a) Cyclic voltammogram and (b) Galvanostatic charge/discharge curve and (c) specific capacitance at various scan rate of activated carbon from waste CD at 900 ˚C for 8 hours.
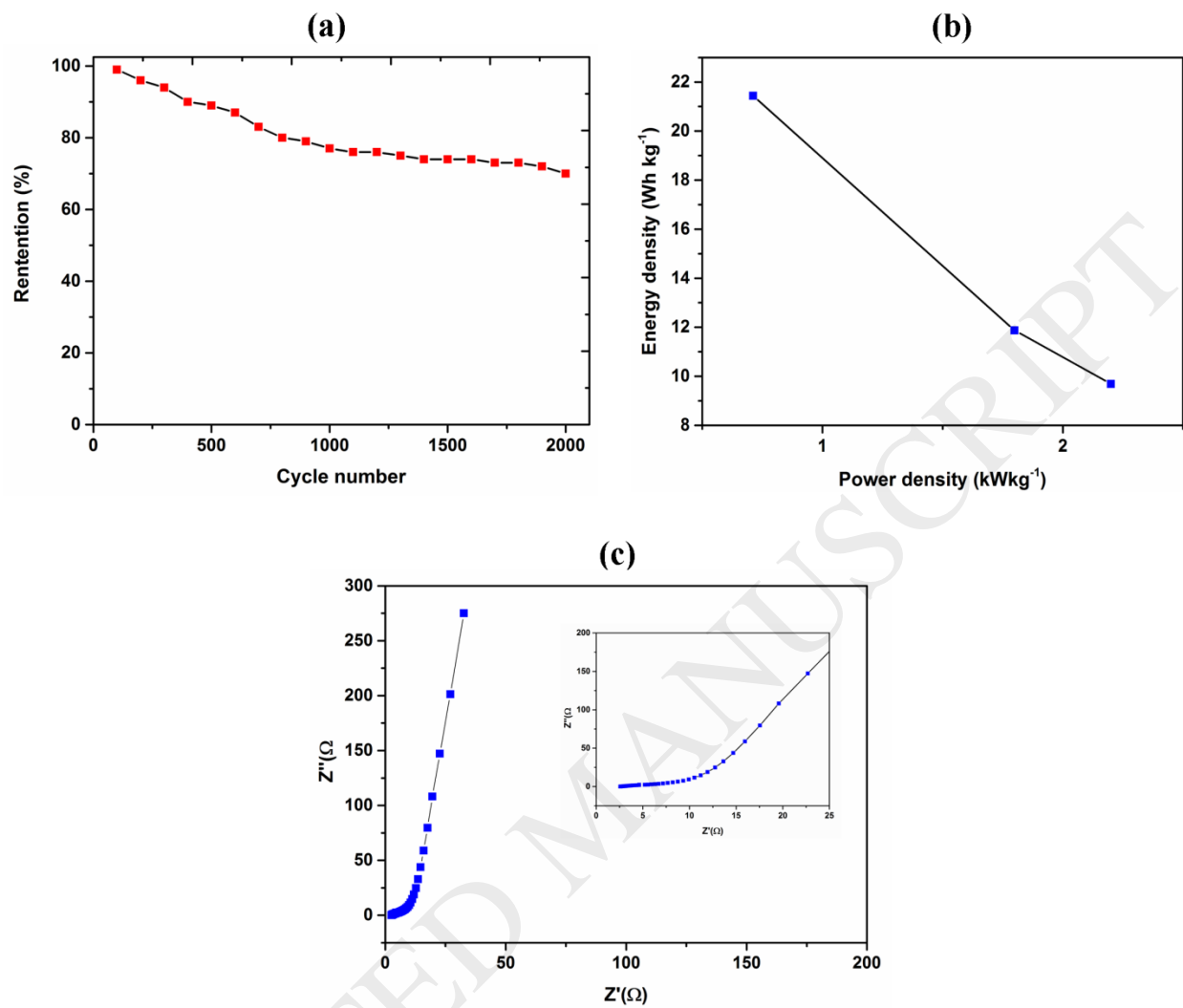
Figure 10: (a) Charge-discharge stability (b) Ragone plots of the energy density and power

density and (c) Nyquist plot of activated carbon obtained from waste CDs.

Table 1: Ultimate, proximate and XRF analysis results of waste CD.

Composition (wt%)	
Ultimate analysis	**Sulphur**
Total Carbon	76.03
Oxygen	20.62
Nitrogen	0.21
Proximate analysis	
Fixed Carbon	19.77
Volatiles	77.99
Moisture	0.22
Ash	2.02
XRF analysis	
F	0.914
Na	0.036
Mg	0.044
Al	0.070
Si	2.160
P	0.007
S	0.028
Cl	0.074
Ca	0.750
Fe	0.058
Ni	0.004
Br	0.005
Ag	0.142
Bi	0.004

Table 2: XPS peak table of prepared activated carbon from waste CD (900 ˚C, 8 hours).

Name	Start BE	Peak BE	End BE	FWHM eV	Area (P) CPS.eV	Atomic %	Total
C1s A	294.58	284.44	281.28	0.9	43759.92	48.54	Atomic % of Carbon is 95.08
C1s B	294.58	284.94	281.28	1.54	24377.97	27.04	
C1s C	294.58	286.54	281.28	1.54	7224.66	8.02	
C1s D	294.58	287.94	281.28	1.54	2974.98	3.3	
C1s E	294.58	289.14	281.28	1.54	3056.26	3.39	
C1s F	294.58	290.83	281.28	1.92	4316.13	4.79	
O1s A	537.98	533.36	526.88	1.92	4916.87	1.95	Atomic % of Oxygen is 4.52
O1s B	537.98	530.54	526.88	1.92	1406.14	0.56	
O1s C	537.98	532.04	526.88	1.92	5060.03	2.01	
Si2p A	104.48	101.73	98.28	1.35	334.66	0.41	Atomic % of Silicon is 0.41

Table 3: Comparison chart of activated carbon for supercapacitors in non-aqueous electrolyte.

Material	S_{BET} $(m^2\,g^{-1})$	C_{sp} $(F\,g^{-1})$	Reference
Melamine resin	442	37	[50]
Polyethylene terephthalate	772	69	[51]
Rice husk	770	19	[52]
Carbon molecular sieve	665	49	[42]
Anthracite	726-1452	18-114	[49]
Lignite	884	65	[49]
Waste CD	1214	51	This work